

ATLAS inner detector material studies

Kerstin Tackmann for the ATLAS Collaboration

CERN, 1211 Geneva 23, Switzerland

DOI: <http://dx.doi.org/10.3204/DESY-PROC-2010-01/195>

A good understanding of the material budget of the ATLAS Inner Detector is crucial for physics analyses at ATLAS. This note describes three complementary studies of the material located inside of the ATLAS electromagnetic calorimeter, using converted photons, uniformity of the energy flow in the electromagnetic calorimeter, and reconstructed K_S mass variations.

1 Introduction

An accurate and high-granularity map of the ATLAS Inner Detector (ID) material is necessary for a precise reconstruction of high-energy photons and electrons. The ID material affects both the track trajectories (especially through bremsstrahlung effects) and the electromagnetic shower development (because of the magnetic field and the energy lost in the ID material). The data taken with the ATLAS detector, described in detail in [1], in the last months of 2009 at a center-of-mass energy of $\sqrt{s} = 900$ GeV and since April of 2010 at $\sqrt{s} = 7$ TeV have allowed for a range of studies, which are complementary in both the reconstruction techniques and the location of the material that is probed.

2 Inner detector studies with converted photons

Reconstruction of converted photons in the ID Low- p_T neutral mesons provide an abundant source of converted photons. They are reconstructed from two oppositely charged tracks with transverse momentum $p_T > 500$ MeV, which have a significant fraction of high-threshold hits in the Transition Radiation Tracker (TRT) as expected for electrons [2]. Several geometric selection criteria and a requirement on the fit quality of the conversion vertex are imposed to remove combinatorial background, while retaining a high signal efficiency.

Material studies To achieve a very high purity, photon conversions are required to have a small vertex fit χ^2 , $\chi_{\text{vtx}}^2 < 5$, and both tracks are required to have at least 4 hits in the silicon Pixel and SemiConductor Tracker (SCT) and at least 90% probability to be electrons, as determined using high-threshold radiation in the TRT. The expected purity from simulation is well above 90% in most regions of the ID and the radial resolution for the vertex position is around 4 mm. About 85000 photon conversion candidates are reconstructed in the $500 \mu\text{b}^{-1}$ that are used for this study. The distribution of photon conversion vertices can be used to map the distribution of material in the ID. Fig. 1 shows clearly the beam pipe ($R = 34.3$ mm), the three barrel Pixel layers ($R = (50.5, 88.5, 122.5)$ mm) and the first two SCT barrel layers

($R = (299, 371)$ mm), together with the Pixel Support Tube ($R = 229$ mm) and various other support structures. In the xy projection, the cooling pipes on the Pixel detector modules and the overlap regions in the first SCT layer are visible. A clear shift in the simulated radial positions is observed for the Pixel Support Tube and global Pixel supports (around $R = 200$ mm) (see Fig. 1 (right)), while the overall amount of material seems to be in good agreement.

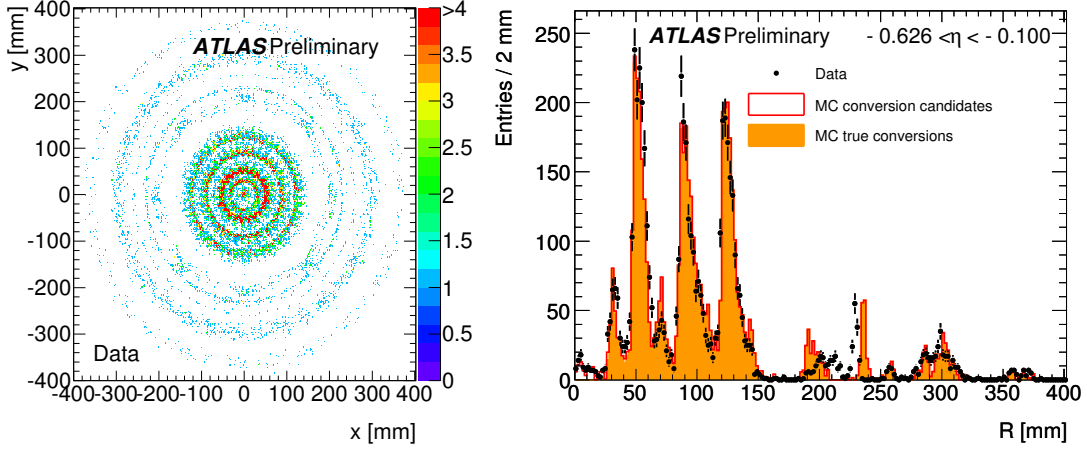


Figure 1: Distribution of reconstructed photon conversion vertices in the xy projection, restricted to $|\eta| < 1$ (left) and radial distribution of reconstructed photon conversion vertices for $-0.626 < \eta < -0.1$ (right).

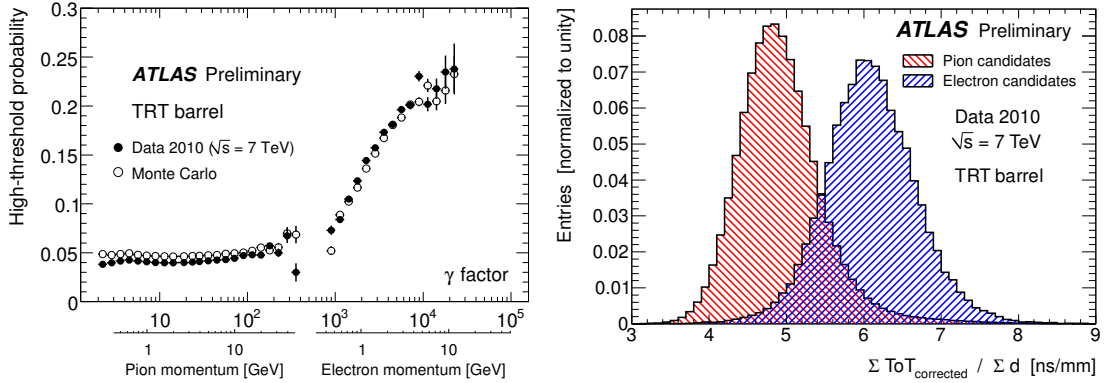


Figure 2: High-threshold onset curve for the barrel region of the TRT (left) and normalized time-over-threshold distributions for electron and π candidates in the TRT barrel region.

Electron identification with the transition radiation tracker Photon conversions can serve as a clean source of electrons for studying the particle identification capabilities of the TRT. The high-threshold radiation onset curve (Fig. 2 left) is determined using a tag-and-probe approach, where, after requiring $\chi^2_{\text{vtx}} < 5$ and at least 4 silicon hits on both tracks, one of the daughter tracks is required to have a fraction of high-threshold hits of more than 0.12, while

the other track is used to extract the rise and the upper plateau of the onset curve. The lower plateau is extracted from generic tracks depleted in electron candidates by requiring a hit in the innermost Pixel layer and vetoing tracks overlapping with photon conversion candidates. The measured time-over-threshold (ToT), normalized to the transverse track length in the straws, yields separation between electrons and hadrons due to the higher ionization energy loss, and hence longer pulses above threshold, of electrons, as shown in Fig 2 (right). Using only low-threshold hits for determining the ToT allows for additional electron-hadron separation independent of the high-threshold information. Electron candidates for this study are supplied by photon conversions with the same selection as used for the material studies.

Cross checking of the beam pipe material using π^0 Dalitz decays

Making use of the well-measured branching fraction of the π^0 Dalitz decay, $\pi^0 \rightarrow e^+e^-\gamma$, the radiation length in a certain volume can be determined by comparing the number of photon conversions in that volume with the number of π^0 Dalitz decays. In particular, this can be used to check the radiation length of the beam pipe, where the efficiency to reconstruct converted photons is almost identical to the efficiency of reconstructing the e^+e^- pairs of Dalitz decays. The relative amount of reconstructed Dalitz decays and photon conversions on the beam pipe is in good agreement between the data and the simulation (see Fig. 3), which gives confidence in the description of the beam pipe in the simulation. In the future, the estimation of the radiation length of the ID material will be done relative to the well-known radiation length of the beam pipe.

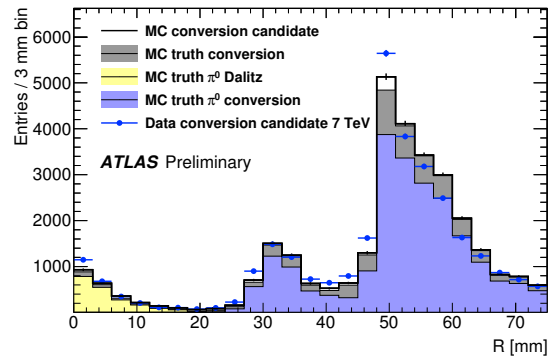


Figure 3: Radial distribution of reconstructed Dalitz decay e^+e^- pairs and photon conversion vertices in the full η range, $|\eta| < 2.5$.

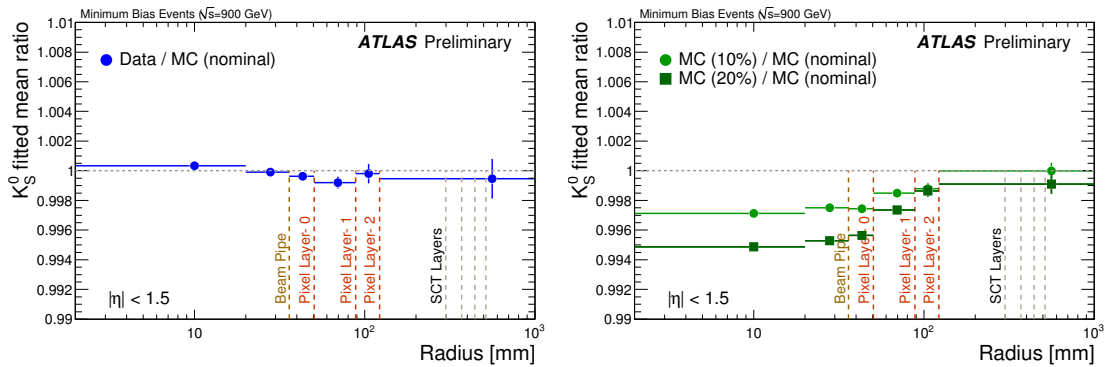


Figure 4: Mean value of the reconstructed K_S^0 mass (normalized to its value reconstructed in the simulation) as a function of the decay radius in data (left) and in simulation samples with additional material (right), which demonstrates the sensitivity of this method.

3 Inner detector material studies with K_S^0

The reconstructed mass of K_S^0 mesons decaying to $\pi^+\pi^-$ is sensitive to the amount of material traversed by the π tracks through their interaction with the detector material through ionization. Flaws in the modeling of the material will result in biased track momenta and hence a biased reconstructed mass of the K_S^0 . By studying the dependence of the reconstructed K_S^0 on the K_S^0 vertex position in radius, η and ϕ , the material in different detector regions can be constrained. Using the $\sqrt{s} = 900$ GeV data taken in 2009, no evidence for unaccounted for material in the Pixel detector up to $|\eta| < 2$ is found and the nominal detector model is found to be a good description of the data [3] (see Fig 4).

4 Probing the material in front of the calorimeter using energy flow in minimum bias events

The occupancy in the electromagnetic (EM) calorimeter is sensitive to the total amount of material in front of the calorimeter. In particular, material outside of the reach of the ID-based methods can be studied with this method. This study [4] uses about $100 \mu\text{b}^{-1}$ collected at $\sqrt{s} = 7$ TeV. The occupancy is defined as the fraction of events with a channel energy above a fixed threshold, which corresponds to about 5 times the electronic noise. Material localized in regions of ϕ can be seen by studying occupancy variations in ϕ at constant η . The amount of material in SCT and TRT services running at constant ϕ and amounting to about $0.2X_0$ is found to be in good agreement between data and simulation. Up to $1X_0$ of material missing in the simulation is observed in the regions around the rails that support the ID, as shown in Fig. 5.

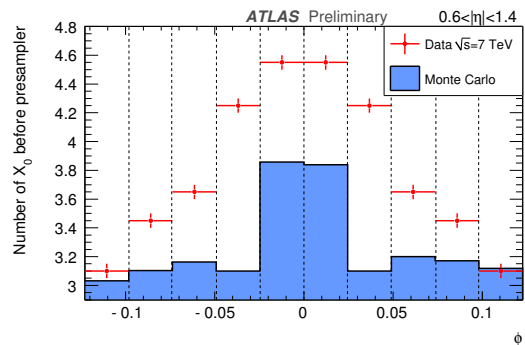


Figure 5: Average number of radiation length X_0 in front of the the EM calorimeter per bin in ϕ ($\Delta\phi = 2\pi/256$, given by the granularity of the cells in the second layer of the EM calorimeter).

5 Conclusions

Multiple complementary methods are used to understand the material budget of the ATLAS Inner Detector. In general, the simulation is found to be in good agreement with the data, with a few localized disagreements.

References

- [1] G. Aad *et al.* [ATLAS Collaboration], JINST **3**, S08003 (2008).
- [2] G. Aad *et al.* [The ATLAS Collaboration], arXiv:0901.0512 [hep-ex].
- [3] The ATLAS Collaboration, ATLAS-CONF-2010-019.
- [4] The ATLAS Collaboration, ATLAS-CONF-2010-037.